A new analytical model for pressure estimation of symmetrical water impact of a rigid wedge at variable velocities

El-M. Yettou*, A. Desrochers, Y. Champoux

Département de génie mécanique, Université de Sherbrooke, 2500 Bd Université, Sherbrooke, Qué., Canada J1K 2R1

Abstract

In this paper we present an analytical solution to symmetrical water impact problems of a two-dimensional wedge. Unlike previous studies, we have taken into account the effect of velocity reduction of the solid body upon impact in order to determine impact pressure as well as the overall force acting on the body. This feature of our study provides a better estimate of the transitory nature of the phenomenon and leads to a more precise evaluation of the true dynamic load borne by the body. We obtained the solution to this problem through a generalization of the Wagner formulation and the use of an existing analytical prediction model of the entry velocity of the wedge. This approach allows us to obtain an original analytical equation for pressure in terms of the kinetics and geometrical parameters of the impact. The validity of the proposed model is demonstrated by a favourable comparison between the analytical results and the physical experiments carried out on several wedge models.
© 2006 Elsevier Ltd. All rights reserved.

Keywords: Wedge; Water impact; Symmetrical; Pressure; Hydrodynamic; Analytical

1. Introduction

Several practical engineering cases require us to consider water impact pressure, as well as to have a working knowledge of water entry dynamics. For example, this is the case for seaplane floats that undergo significant loading during water landing, as well as for high-speed boats that frequently perform wave jumps from considerable heights. Usually, this kind of problem is simplified as a two-dimensional solid dropped vertically onto a free and initially calm water surface. Notwithstanding these simplifications, the solution to this type of problem remains complex, especially with regard to transient fluid–structure interactions.

In 1929, von Karman introduced significant work on this subject. He developed an analytical formula which allows estimation of the maximum pressure on seaplane floats during water landing (von Karman, 1929; Payne, 1988). In 1936, Wagner modified the von Karman solution by taking into account the effect of water splash on the body (Wagner, 1936; Korobkin and Pukhnachov, 1988). This work was further developed by Howison et al. (1991), who introduced the nonlinear effect of the water splash near the intersection point between the body and the water's surface.

---

*Corresponding author. Tel.: +1 819 821 8000x2657; fax: +1 819 821 7163.

E-mail addresses: El-Mahdi.Yettou@Usherbrooke.ca (E.-M. Yettou), Alain.Desrochers@Usherbrooke.ca (A. Desrochers), Yvan.Champoux@Usherbrooke.ca (Y. Champoux).

In the special case of wedges entering water vertically at a constant velocity, Dobrovolskaya (1969) derived a similar solution by making use of the simple geometry of the body. Although this solution is valid for any deadrise angle, it is implicitly provided in terms of integral equations which must be solved numerically.

During the 1980s and following the developments recorded in the field of numerical calculation, several studies were carried out for various increasingly complex impact configurations. To illustrate, we need only cite the works of Armand and Cointe (1987) on a cylinder entering the water at a constant velocity; or the studies carried out by Troesch and Kang (1987, 1990) on the three-dimensional aspect of hydrodynamic impact and flare slamming. They presented theoretical, experimental and numerical results for a sphere and a cusped body which was axisymmetric and resembled the bow profile of a ship with flare.

Zhao et al. (1993, 1996) introduced a complement to Wagner's studies, with linear approximation of the free-surface boundary condition for the two-dimensional impact problem. They solved the linearised problem for wedges and ship bow-flare sections through a numerical procedure based on the boundary integral equation method.

More recently, Mei et al. (1999) proposed a purely analytical method of resolution for the global two-dimensional impact problem of arbitrary bodies. They adopted the same assumptions and the same linearised formulation of the problem as was used by Zhao et al. (1996). Then, they solved the problem analytically using the well-known conformal mapping technique. This technique was adopted early on by several researchers such as Hughes (1972), who developed a quasi-analytical solution to the classical hydrodynamic problem of the entry at constant velocity of a prismatic wedge into an incompressible inviscid fluid. Fraenkel and McLeod (1997) also applied the conformal mapping method to the boundary value problem formulated by Wagner (1936). They were thus able to derive an explicit solution to the limiting case of an infinite wedge of vertex angle π. Later, Fraenkel and Keady (2004) studied the thin wedge and the problem of the contact angle (the angle formed between the water's free surface and the body's surface at the intersection point). They also used a conformal transformation to solve the problem. More recently, Faltinsen (2002) used this transformation to analyse the water entry of a rigid wedge. In the study by de Divitiis and de Socio (2002), they carried out a distribution of potential singularities in solving the so-called Wagner problem. Further, the conformal transformation technique was adopted to determine the unknown intensities of the discontinuities. These authors studied both the symmetrical and the asymmetrical entries at constant velocity of a wedge-shaped body. Furthermore, it is worthwhile to note that all these results (Mei et al., 1999; Hughes, 1972; Fraenkel et al., 1997, 2004; Faltinsen, 2002; de Divitiis and de Socio, 2002) specifically address the case of an impact at constant velocity.

We should also mention the extensive analytical work that was done by Korobkin on the water impact of a rigid body. His investigation on mathematical models for the prediction of the hydrodynamic pressure distribution and the force on the body is essential (Korobkin, 1997, 2004). Along with Scolan he presented substantial analytical work on three-dimensional water impact (Scolan and Korobkin, 2001; Korobkin and Scolan, 2006).

Finally, we will cite the exhaustive study by Faltinsen et al. (2004) which summarizes the most significant work achieved on the impact phenomenon and its applications to marine engineering.

The study presented in this document draws its inspiration from the work of Mei et al. (1999). However, we focussed on deriving an analytical solution for the general case of a wedge's water impact at variable velocity. We used the same linearised boundary-value formulation as Zhao et al. (1996). Then, we solved the linearised problem analytically using conformal mapping techniques simultaneously with an analytical model predicting the entry velocity of the wedge (Zhao et al., 1996; Mei et al., 1999). We wish to note, however, that the approach we suggest could be extended to the more general case of arbitrary body geometry, through the use of a distinct model to estimate the body's velocity upon impact.

This paper is divided into four sections. In Section 2, we have formulated the linearised boundary-value problem of the symmetrical water impact of a wedge at variable velocity. In Section 3, we have developed an improved analytical solution based on the method suggested by Mei et al. (1999). In Section 4, we have described physical experiments and compared experimental data with analytical results. Finally, our conclusions and comments are presented in Section 5.

2. Formulating the problem

Let us consider the problem of two-dimensional vertical impact at arbitrary velocity of a symmetrical rigid wedge onto an initially calm water surface. The solid body is considered to be symmetrical with respect to its vertical axis. Upon introducing the Cartesian coordinate system (y, z), the y-axis lies on the undisturbed water surface and the z-axis merges with the symmetry axis of the body (see Fig. 1); the body surface is represented by the equation $h = h(y)$, where h denotes the vertical distance between a point on the wedge surface and its apex.
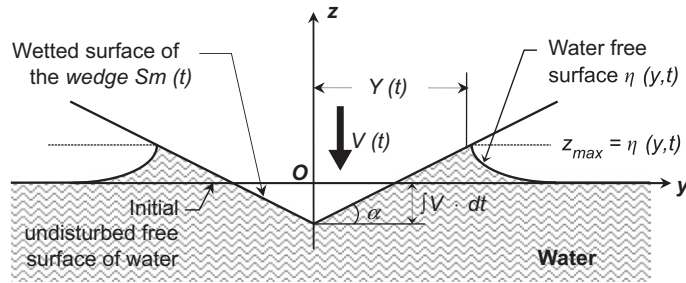
Fig. 1. Parameters involved in the description of the water impact of a wedge at variable velocities.

Considering the nature of the fluid and the mechanism being studied, we assume, as did the majority of the researchers, the following traditional hypotheses: (i) the body is infinitely rigid; (ii) water is considered to be an incompressible and nonviscous fluid; (iii) flow is irrotational; (iv) the effect of possible air trapped between the body and the free surface of the water is negligible; (v) the free surface of the water is initially calm; (vi) gravitational force is negligible compared to the body's inertia; (vii) atmospheric pressure is equal to zero.

Thus, the continuity equation consists in determining a velocity potential $\phi(y, z, t)$ which satisfies the Laplace equation and the boundary conditions described below. This classical formulation of the problem has been stated previously by several researchers (Wagner, 1936; Cappelli and Wilkinson, 1967; Li and Sigimura, 1967; Korobkin and Pukhnachov, 1988). The two free-surface boundary conditions are written in the following form:

the kinematic free-surface boundary condition:

$$\frac{\mathrm{D}\eta}{\mathrm{D}t} = \frac{\partial \phi(y, z, t)}{\partial z} \quad \text{on} \quad z = \eta(y, t), \tag{1}$$

the dynamic free-surface boundary condition:

$$\frac{\mathrm{D}\phi}{\mathrm{D}t} - \frac{1}{2}(\phi_y^2 + \phi_z^2) = 0 \quad \text{on} \quad z = \eta(y, t), \tag{2}$$

where η denotes the vertical coordinate of a point on the water free surface, and $\mathrm{D}/\mathrm{D}t$ denotes the substantial derivative.

The nonlinear terms in these two expressions constitute the major difficulty in solving the boundary value problem in an analytical fashion. However, it is possible to make up for this difficulty by applying a few simplifications and a partial linearisation of the problem. In fact, in his asymptotic solution, Wagner (1936) simplified the dynamic boundary condition thus:

$$\phi(y, z, t) = 0. \tag{3}$$

Then he applied it on the horizontal line that starts at the intersection point between the body and the free surface $Z = \eta(Y, t)$. The kinematic free-surface boundary condition was used to determine the intersection between the free surface and the body. Later, Zhao et al. (1996) and Mei et al. (1999) used this same approach in their analyses. We must stress that the Dirichlet condition (3) is applied to the horizontal plane passing through the intersection point $Z = \eta(Y, t)$ and not on the exact free surface $z = \eta(y, t)$. This particular aspect of the linearised free-surface conditions makes it possible to take into account the significant contribution associated with the wetted body surface above the initially undisturbed water surface. In other words, this allows us to include the effect of the water splash. From there, and by applying these simplifications, the boundary value problem amounts to the determination of the velocity potential $\phi(y,z,t)$, thus satisfying:

the Laplace equation

$$\Delta\phi(y, z, t) = 0, \tag{4}$$

the linearised kinematic free-surface boundary condition

$$\frac{\partial \eta}{\partial t} = \frac{\partial \phi(y, z, t)}{\partial z} \quad \text{on} \quad Z = \eta(Y, t), \tag{5}$$

the linearised dynamic free-surface boundary condition

$$\phi(y, z, t) = 0 \quad \text{on} \quad Z = \eta(Y, t) \tag{6}$$

the kinematic body boundary condition

$$\frac{\partial \phi}{\partial n} = -V(t)n_z \quad \text{on} \quad S_m(t), \tag{7}$$

the far-field condition

$$\left|\nabla \phi\right| \to 0 \quad \text{as} \quad (y^2 + z^2)^{1/2} \to \infty, \tag{8}$$

and *the initial condition*

$$\phi(y, z, 0) = 0 \quad \text{and} \quad \eta(y, 0) = 0 \quad \text{on} \quad z = 0, \tag{9}$$

where $S_m(t)$ represents the instantaneous wetted body surface (see Fig. 1), $V(t)$ is the instantaneous velocity of the wedge upon impact, $\mathbf{n} = (n_y, n_z)$ is the normal unit of the body surface.

It should be noted that the approximations carried out above are not valid for the flow near the apex of the water splash. In this region, the free surface changes its shape sharply and its nonlinearity must be considered. However, we know that the local jet flow is not very relevant from a practical point of view in estimating the impact pressure as well as the slamming force on the body (Zhao and Faltinsen, 1993). We are thus able to ignore the thin-jet flow and consider the global problem.

After obtaining the boundary-value solution and determining the function ϕ, the pressure value can be calculated using Bernoulli's equation:

$$p = -\rho \left(\phi_t + \frac{1}{2} \left|\nabla \phi\right|^2 \right), \tag{10}$$

where ρ is the fluid density.

However, unlike the case studied by Zhao and Faltinsen (1993) and Mei et al. (1999), the instantaneous velocity of the wedge $V(t)$ is unknown in our case. Thus, in order to solve the linearised boundary-value problem, we first need to evaluate the velocity variation of the wedge upon impact. This is made possible by applying the momentum theorem,

$$V(t) = \frac{V_0}{1 + M_a/M}, \tag{11}$$

where $V(t)$ is the instantaneous velocity of the wedge upon impact, V_0 is the initial falling velocity of the wedge (at $t = 0$), M is the mass of the wedge, M_a is the added mass of the wedge.

The added mass of the wedge is calculated using the commonly used form (Zhao et al., 1996; Mei et al., 1999)

$$M_a = C_a \rho (Y(t))^2, \tag{12}$$

where

$$C_a = \frac{\delta \pi}{2} \left(1 - \frac{\alpha}{2\pi} \right)^2; \tag{13}$$

$Y(t)$ represents the horizontal coordinate of the intersection point between the body and the free surface (see Fig. 1), α is the deadrise angle of the wedge, and δ is a correction factor taking into account the three-dimensional effects associated with the non infinitely-long bodies used in the experiments. The factor δ is obtained according to the suggestions made by Zhao et al. (1996). It varies from 0.5 to 1, depending on the geometry of the body involved in the impact [for further details about this correction factor, we advise readers to refer directly to Zhao et al. (1996), Meyerhoff (1970) and Yu (1945)]. Just as Zhao et al. (1996) and Mei et al. (1999), in order to compare analytical results to experimental data, the factor δ will be considered in Eq. (13) to determine the analytical value of the coefficient Ca which will be used in Eq. (12) to determine the value of the added mass M_a.

Equations (11)–(13) expressing the instantaneous velocity of the wedge and the added mass of the wedge are not new equations. They have been used before by several researchers [e.g., Zhao et al. (1996) and Mei et al. (1999)] to estimate the body's velocity upon impact. In this study, we will also use them to determine the instantaneous velocity of the wedge and hence in solving the linearised boundary value problem stated above. However, Eq. (11) is given in terms of the horizontal coordinate $Y(t)$ of the intersection point between the water's surface and the wedge side which is *a priori* unknown. Nevertheless, for bodies with smooth surfaces like wedges, this variable can be expressed analytically with the help of some polynomial approximations.

3. Analytical solution

3.1. Extension of previously obtained analytical results

In this section, we will extend the work of Mei et al. (1999) to include the more general case of variable velocity of a wedge. In this case, we will use the same approach as the aforementioned authors. However, we re-emphasise that, unlike the case studied by Mei et al. (1999), the effect of the variation of the body velocity will be taken into account in determining instantaneous pressure distribution.

Consequently, as the application of the Dirichlet condition $\phi = 0$ on the free surface $Z = \eta(Y, t)$ suggests an antisymmetry of the velocity potential $\phi(y,z,t)$ with respect to this plane, the hydrodynamic images method and conformal mapping technique are applied to the problem. The linearised boundary value problem can therefore be considered as a rhombus moving in an infinite fluid field with a velocity $V(t)$ corresponding to the actual velocity of the wedge. This fictitious rhombus is made of the immersed segment of the real wedge and its symmetrical image around the plane $Z = \eta(Y, t)$. Its width depends on the value of $Y(t)$ (see Fig. 2).

Since we are reintroducing this problem to a well-known hydrodynamic scenario, it is useful to apply the following transformation:

$$y' = y, \tag{14}$$

$$z' = z - \eta(Y, t), \tag{15}$$

where

$$\phi(y, z, t) = \phi'(y', z', t) - V(t)z'. \tag{16}$$

The conformal mapping technique is well suited to solving this kind of problem. By means of the mapping technique, the unknown flow parameters in the physical plane will have a well-known correspondence to the complex plane. As suggested by several researchers such as Hughes (1972), Fraenkel and McLeod (1997) and others, we will use the Schwartz–Christoffel transformation which makes it possible to represent the flow with a velocity $V(t)$ through a rhombus in the physical plane ($Z = y' + \mathrm{i}z'$) by a vertical flow with a velocity $U(t)$ in the mapped plane ($W = p + \mathrm{i}q$) (see Fig. 3).

The relation between Z and W is expressed by

$$\frac{Z}{Y(t)} = A^{-1} \int_0^W \left(\frac{w^2}{w^2 + 1}\right)^\theta \mathrm{d}w + 1, \tag{17}$$

where

$$A = \cos \alpha \int_0^1 \left(\frac{w^2}{1 - w^2}\right)^\theta \mathrm{d}w \tag{18}$$

and

$$\theta = \frac{(\pi - 2\alpha)}{2\pi}. \tag{19}$$
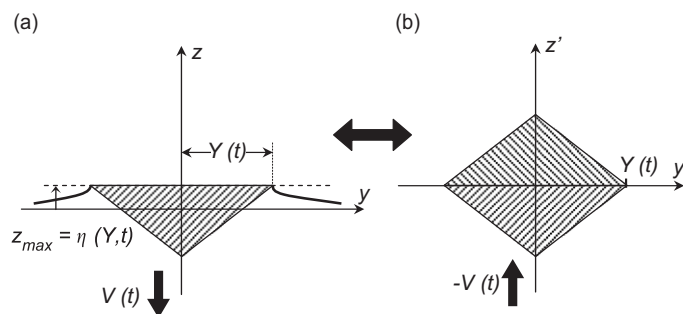
Fig. 2. Symmetry and flow analogy principles.
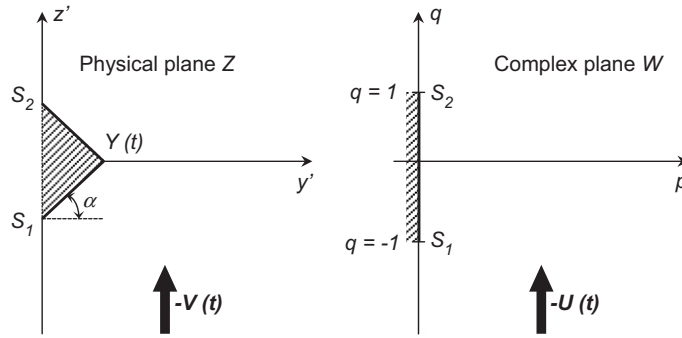
Fig. 3. Representation of the impact of a *wedge* in the complex plane W according to the Schawrtz–Christoffel transformation.

In the complex plane, the velocity potential is a known entity (Newman, 1977):

$$\phi'(y', z', t) \equiv \Phi(Z, t) = \mathscr{R}e\{-iW\}\frac{V(t)\,Y(t)}{A}.$$ (20)

The complex velocity of the flow can be obtained using transformation (17):

$$u - iv = \frac{\partial \Phi}{\partial y'} - i\frac{\partial \Phi}{\partial z'} = -iV(t)\,Y(t)A^{-1}\frac{dW}{dZ} = -iV(t)\left(\frac{W^2 + 1}{W^2}\right)^{\theta}.$$ (21)

When referring to situation (B) of Fig. 2 and to Eqs. (17) and (20), it appears obvious that the solution to the problem is based on determining the exact geometry of the rhombus. In other words, to solve the problem analytically, we need to know the time variation of the position at the intersection point $Y(t)$.

For this purpose, we have used the very interesting method proposed by Mei et al. (1999). These authors developed a polynomial expression of the height $H(Y)$ of the intersection point $(Y(t), \eta(Y))$ measured from the apex of the wedge. This expression was used to obtain a polynomial relation between $Y(t)$ and the constant velocity of the wedge. In our case, although the speed of the wedge is variable, the Mei et al. method might be used to obtain another relation between $Y(t)$ and $V(t)$ and hence, together with Eq. (11), it is possible to determine the two unknown variables, i.e. $Y(t)$ and $V(t)$.

Since the aim of this paper is not to reproduce the work of Mei et al. (1999), we have provided a brief description of the main steps of Mei's method (see below). For further details, readers are referred directly to Mei et al. (1999).

The authors of that study made use of the governing equation for the motion of the intersection point $Y(t)$ to express $H(Y)$ in terms of the speed of the body and the vertical component of the velocity of the water's surface at the intersection point $Y(t)$. Then they introduced the variable $\mu(Y)$ which is defined by $\mu(Y) = V_0 dt/dY$. We should note here that for the case studied by Mei et al. (1999), the speed of the body V_0 is constant and well known at any time during the impact process. In spite of this, we are nevertheless able to obtain the same relation for $\mu(Y)$; however, instead of a constant speed V_0, we have a variable speed $V(t)$ that can be determined using Eq. (11).

Since the solid studied by Mei et al. (1999) was (as in our case) a rigid wedge whose surface can be described by a continuous function, they could therefore suppose that the intersection point $Y(t)$ moves along the body surface in a continuous manner. This enabled them to use the polynomial expansion of Chebyshev applied to the N first terms to describe $\mu(Y)$. This approximation is also valid for the case where the speed of the body $V(t)$ is variable, so we used the same approach as Mei et al. (1999) to obtain:

$$\mu(Y) = V(t)\frac{dt}{dY} = \sum_{n=0}^{N-1} b_n Y^n.$$ (22)

By integrating the expression above, we obtained the following relation between the quantity $\int_0^t V\,dt$ and $Y(t)$:

$$\int_0^t V\,dt = \sum_{n=0}^{N-1} \frac{b_n}{n+1} Y^{n+1}.$$ (23)

To determine the progression of the intersection point $Y(t)$ together with the instantaneous velocity of the wedge $V(t)$, we need to solve the following system of equations:

$$V(t) = \frac{V_0}{1 + C_a \rho (Y(t))^2 / M}, \quad \int_0^t V \, dt = \sum_{n=0}^{N-1} \frac{b_n}{n+1} Y^{n+1}. \tag{24}$$

However, prior to this we first need to establish the value of the unknown coefficients b_n. For this, we used the Schwartz–Christoffel transformation properties. Since a variable speed does not introduce any changes to the determination of the unknown coefficients b_n, we obtain, like Mei et al. (1999), the same result for the coefficient b_n:

$$b_0 = \frac{\tan(\alpha)}{\gamma} \quad \text{and} \quad b_n = 0 \text{ for } n \neq 0, \tag{25}$$

where α is the deadrise angle of the wedge; γ denotes a dimensionless parameter that depends solely upon the deadrise angle of the wedge; it measures the water's splash onto the wedge. It can be provided directly from the following equation obtained by Mei et al. (1999):

$$\gamma(\alpha) = A(\alpha) \int_0^1 \left[\int_0^p \left(\frac{w^2}{w^2+1} \right)^\theta dw + A(\alpha) \right]^{-2} dp. \tag{26}$$

By replacing the values of the coefficients b_n in Eq. (23), we finally obtain the time variation of the position of the intersection point $Y(t)$ in relation to the velocity $V(t)$:

$$Y(t) = \frac{\gamma}{\tan(\alpha)} \int_0^t V(t) \, dt. \tag{27}$$

In the Mei et al. model, the velocity of the wedge V_0 is known and constant. The position of the intersection point $Y(t)$ can thus be obtained directly from the following equation [see Mei et al. (1999)]:

$$Y(t) = \frac{\gamma(\alpha)}{\tan(\alpha)} V_0 t. \tag{28}$$

For the case studied in this paper, the velocity of the wedge is unknown and variable over time. However, it is possible to determine it simultaneously with the position of the intersection point $Y(t)$. This can be done using the following system formed by Eqs. (11) and (27):

$$V(t) = \frac{V_0}{1 + (C_a \rho (Y(t))^2 / M)}, \quad Y(t) = \frac{\gamma}{\tan(\alpha)} \int_0^t V(t) \, dt. \tag{29}$$

It is then possible to observe that the position of the intersection point $Y(t)$ can be evaluated from the same equations obtained in the particular case of the impact at constant velocity (Mei et al., 1999). The only difference lies in estimating the penetration depth of the wedge from the initially undisturbed water surface. In the case of constant velocity, this depth is expressed by the quantity $(V_0 t)$ where V_0 represents the constant velocity of the wedge. On the other hand, in the case of a variable velocity, this depth is more exactly expressed by $\int_0^t V(t) \, dt$.

The analytical solution to the above equation set leads to the solution of a nonlinear differential equation of the first order for the unknown intersection point $Y(t)$,

$$\frac{dY(t)}{dt} - \frac{\gamma(\alpha) M V_0}{\tan(\alpha) \left(M + C_a \rho (Y(t))^2 \right)} = 0. \tag{30}$$

This equation can be further simplified to obtain

$$\frac{\rho C_a}{3} (Y(t))^3 + M Y(t) - \frac{\gamma M V_0}{\tan(\alpha)} t = 0. \tag{31}$$

It is worthwhile to note that Mei et al. (1999) introduced Eq. (31) to estimate the time variation of the external force on the body for the impact of a free-falling wedge into water. For this purpose, they used the following equation:

$$\frac{dY}{dt} = \frac{\gamma(\alpha)}{\tan(\alpha)} V. \tag{32}$$

The above equation was derived from Eq. (28), by replacing V_0 with V. As well, it should be remembered that Eq. (28) was obtained specifically for the case of a constant wedge speed. Then, to obtain Eq. (31), they combined Eq. (32) with Eq. (11), which implicitly gives the time variation of the body's speed in terms of the intersection point $Y(t)$. Although

the result obtained is completely accurate, as noted by the system of equations (29), the authors unfortunately did not provide any explanation regarding the combination of two apparently nonhomogenous equations, since Eq. (28) (derived from Eq. (32)) is used for constant impact velocity and Eq. (11) for variable impact velocity [see Mei et al. (1999)]. Neither did they analyse the effect of the variation of the wedge speed on pressure distribution. Consequently, we will present the effect of such a variation on the pressure estimation and compare it with Mei's model (see below).

As stated in Section 2, to determine the instantaneous pressure distribution on the surface of the wedge, we must replace the solution ϕ of the boundary value problem in Bernoulli's equation (10). To do this, as we have demonstrated, the speed $V(t)$ and the position of the intersection point $Y(t)$ must be determined. This can be carried out using the system of equations (29). However, the analytical solution to this system might lead to a lengthy expression of $Y(t)$ and thus an unwieldy expression of $V(t)$. This tends to complicate the equations of the pressure distribution, making them difficult to use. We therefore prefer solving the system in a numerical fashion. This is possible using any classical method of numerical integration, such as Simpson's method.

3.2. Determination of the pressure distribution

With $Y(t)$ and $V(t)$ as known entities, we can now replace them by their respective values in Eq. (20) to determine the expression of the velocity potential ϕ. Next, to obtain the distribution of pressure on the wedge, we simply need to introduce the value of ϕ in Bernoulli's equation.

The pressure at any given point on the wedge in terms of the velocity potential ϕ is expressed by

$$\frac{P(y,z,t)}{\rho} = -\frac{\partial \phi}{\partial t} - \frac{1}{2}\left[\left(\frac{\partial \phi}{\partial y}\right)^2 + \left(\frac{\partial \phi}{\partial z}\right)^2\right] = -\frac{\mathrm{D}\phi}{\mathrm{D}t} - V(t)\frac{\partial \phi}{\partial z} - \frac{1}{2}\left[\left(\frac{\partial \phi}{\partial y}\right)^2 + \left(\frac{\partial \phi}{\partial z}\right)^2\right]. \tag{33}$$

By introducing variables ϕ', y' and z' defined by Eqs. (14)–(16) and knowing that

$$\frac{\mathrm{D}z}{\mathrm{D}t} = -V(t) \text{ and } \eta(Y,t) = H(Y) - \int_0^t V \, \mathrm{d}t,$$

Eq. (33) becomes

$$\frac{P(y',z',t)}{\rho} = -\frac{\mathrm{D}\phi'}{\mathrm{D}t} - \frac{1}{2}\left[\left(\frac{\partial \phi'}{\partial y'}\right)^2 + \left(\frac{\partial \phi'}{\partial z'}\right)^2\right] - V(t)\frac{\mathrm{D}H(Y)}{\mathrm{D}t} + \frac{1}{2}(V(t))^2 + z'\frac{\mathrm{D}V(t)}{\mathrm{D}t}. \tag{34}$$

Introducing the dimensionless pressure coefficient C_p, we obtain

$$C_p = 2\frac{P(y',z',t)}{\rho(V(t))^2} = \left\{-\frac{2}{(V(t))^2}\frac{\mathrm{D}\phi'}{\mathrm{D}t} - \frac{1}{(V(t))^2}\left[\left(\frac{\partial \phi'}{\partial y'}\right)^2 + \left(\frac{\partial \phi'}{\partial z'}\right)^2\right] - \frac{2}{V(t)}\frac{\mathrm{D}H(Y)}{\mathrm{D}t} + 1\right\}$$
$$+ \left\{\frac{2z'}{(V(t))^2}\frac{\mathrm{D}V(t)}{\mathrm{D}t}\right\}. \tag{35}$$

Using Eqs. (20), (21) and (27) we can now rewrite Eq. (35) in terms of the parameters of the complex plane W:

$$C_p = \underbrace{\left\{\frac{2\gamma}{A\tan(\alpha)}\left[\left(\frac{1-q^2}{q^2}\right)^\theta \int_{|q|}^1 \left(\frac{w^2}{1-w^2}\right)^\theta \mathrm{d}w - q\right] - \left(\frac{1-q^2}{q^2}\right)^{2\theta} - 2\gamma + 1\right\}}_{C_{p_{\mathrm{Mei}}}}$$
$$+ \underbrace{\left\{\frac{2\gamma}{A\tan(\alpha)}\left[\sin(\alpha)\int_0^q \left(\frac{w^2}{1-w^2}\right)^\theta \mathrm{d}w - q\right]\int_0^q V(t)\,\mathrm{d}t\frac{\mathrm{D}V(t)}{\mathrm{D}t}\frac{1}{(V(t))^2}\right\}}_{\Delta C_p}. \tag{36}$$

We now observe that the pressure coefficient represents the sum of two terms $C_{p_{\mathrm{Mei}}}$ and ΔC_p. The term $C_{p_{\mathrm{Mei}}}$ represents the pressure coefficient obtained by Mei et al. (1999) for the particular case of wedges entering water vertically at a constant velocity. Thus, the additional term ΔC_p expresses the difference between the pressure coefficient in this particular case (impact at constant velocity) and that of the more general case of a variable velocity. It should

also be noted that, unlike $C_{p_{\text{Mei}}}$ which depends only on the body geometry, ΔC_p depends on the variation of the wedge's velocity in a non linear fashion. It represents the effect of the wedge's deceleration on pressure distribution.

Finally, the total slamming force can be obtained by directly integrating pressure distribution with respect to the wetted surface of the wedge:

$$F(t) = 2 \cos(\alpha) \int \int_{S(t)} P(l, t) \, \mathrm{d}S = 2 \cos(\alpha) \int_0^{Y(t)} P(l, t) \, \mathrm{d}l; \tag{37}$$

or by applying Newton's second law,

$$F(t) = M \frac{\mathrm{d}(V(t))}{\mathrm{d}t}, \tag{38}$$

where $V(t)$ is the velocity of the wedge given by Eq. (11), M is the mass of the wedge.

3.3. Analysis of the variation of the pressure coefficient

We present below a brief study of the time variation of the dimensionless terms $C_{p_{\text{Mei}}}$ and ΔC_p as well as their sum, i.e. coefficient C_p provided by Eq. (36). The effects of some slamming parameters such as the mass of the body, the drop height and the deadrise angle of the wedge are also analysed.

The following curves are plotted in terms of the dimensionless entry depth ξ which represents the ratio of the height, measured from the apex, of a given point on the wetted part of the wedge surface, to the penetration depth of the wedge around the initially undisturbed water surface expressed by the integral $\int_0^t V(t) \, \mathrm{d}t$. In other words,

$$\xi = \frac{h(l, t)}{\int_0^t V(t) \, \mathrm{d}t} \quad \text{with} \quad 0 \leqslant l \leqslant Y(t); \tag{39}$$

hence

$$\frac{h(0, t)}{\int_0^t V(t) \, \mathrm{d}t} \leqslant \xi \leqslant \frac{h(Y, t)}{\int_0^t V(t) \, \mathrm{d}t} \quad \text{thus} \quad 0 \leqslant \xi \leqslant \gamma. \tag{40}$$

Fig. 4 shows the time variation of the dimensionless quantities C_p, $C_{p_{\text{Mei}}}$ and ΔC_p. It would appear that the absolute value of ΔC_p which represents the difference between the pressure coefficients C_p and $C_{p_{\text{Mei}}}$, increases over time. However, this variation becomes very weak near the peak pressure point (at $\xi \approx 1.54$) and at the wedge apex (at $\xi = 0$). The effects of the variation of the mass and drop height are very small and may be set aside as shown in Figs. 5 and 6.

Fig. 7 illustrates the effect of the deadrise angle of the wedge on C_p, $C_{p_{\text{Mei}}}$ and ΔC_p. It is evident that the smaller the deadrise angle α, the stronger and shorter the peak. This was noticed previously by several researchers such as
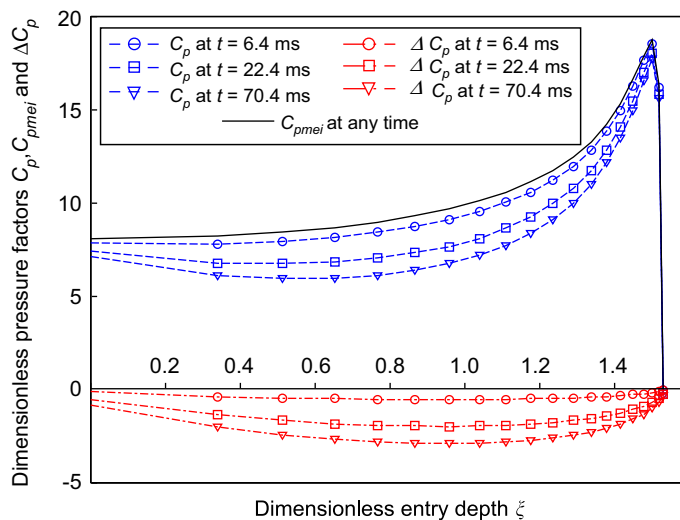
Fig. 4. Time variation of dimensionless pressure factors C_p, ΔC_p and $C_{p_{\text{Mei}}}$ (wedge deadrise angle $\alpha = 20°$; wedge mass $m = 200 \, \text{kg}$; drop height $hc = 2 \, \text{m}$).
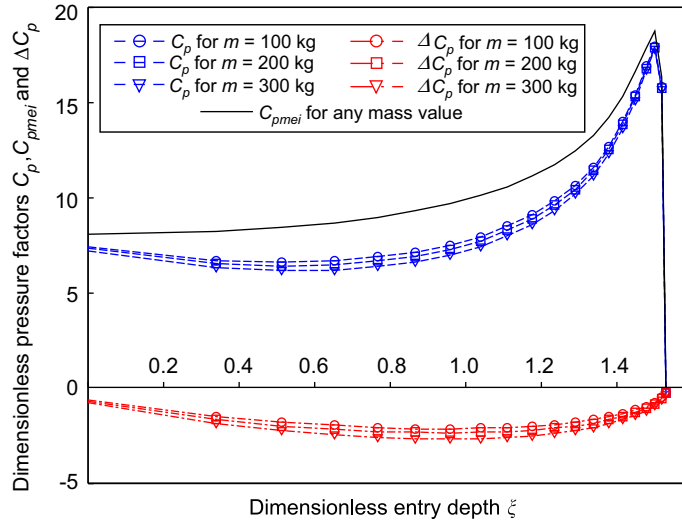
Fig. 5. Effect of the body's mass on the dimensionless pressure factors C_p, ΔC_p and $C_{p_{\text{Mei}}}$ (wedge deadrise angle $\alpha = 20°$; drop height $hc = 2$ m; curves plotted at $t = 32$ ms).
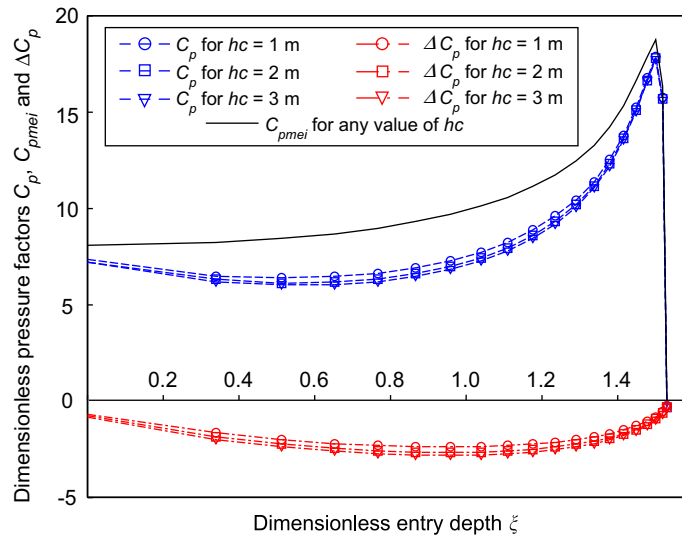
Fig. 6. Effect of the drop height on the dimensionless pressure factors C_p, ΔC_p and $C_{p_{\text{Mei}}}$ (wedge deadrise angle $\alpha = 20°$; wedge mass $m = 200$ kg; curves plotted at $t = 48$ ms).

Dobrovolskaya (1969), Zhao and Faltinsen (1993) and others. In addition, it is also possible to note that the smaller the angle α, the larger the value of ΔC_p, and therefore the greater the difference between C_p and $C_{p_{\text{Mei}}}$. However, the fact remains that close to the peak pressure point and in the vicinity of the wedge's apex, this variation is very weak. This discrepancy near the peak pressure point is about 1–10% of the value of $C_{p_{\text{Mei}}}$ depending on the deadrise angle of the wedge. Consequently, it is completely acceptable to set ΔC_p aside and to consider the simplified formula, as expressed by Eq. (41), for the prediction of the maximum value of the pressure coefficient C_p in the case of wedges entering water vertically at variable velocities:

$$C_{p_{\max}} = \left\{ \frac{2\gamma}{A \tan(\alpha)} \left[\left(\frac{1-q^2}{q^2} \right)^{\theta} \int_{|q|}^{1} \left(\frac{w^2}{1-w^2} \right)^{\theta} dw - q \right] - \left(\frac{1-q^2}{q^2} \right)^{2\theta} - 2\gamma + 1 \right\} \quad \text{for} \quad q = 0. \tag{41}$$
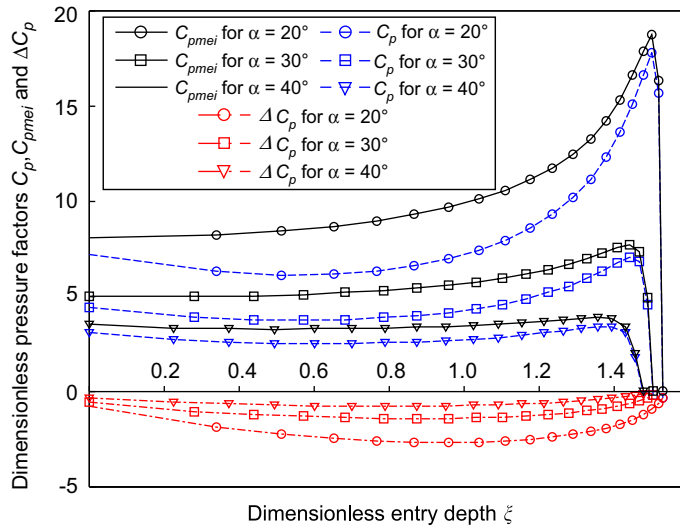
Fig. 7. Effect of the deadrise angle of the wedge on the dimensionless pressure factors C_p, ΔC_p and $C_{p_{\text{Mei}}}$ (mass of the wedges $m = 200\,\text{kg}$; drop height $hc = 2\,\text{m}$; curves plotted at $t = 48\,\text{ms}$).
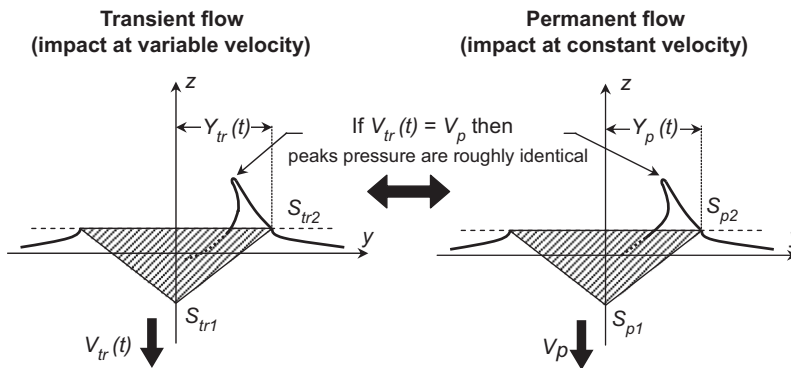
Fig. 8. Analogy between permanent and transient flow for the wedge's water impact.

Eq. (41) is of course limited to the prediction of the maximum value of the pressure coefficient which allows, upon evaluation, a determination of the peak pressure value by using the following well-known formula:

$$P(Y, z_{\max}, t) = \frac{\rho(V(t))^2}{2} C_{p_{\max}}. \tag{42}$$

However, Eq. (41) cannot be used to evaluate the pressure distribution elsewhere on the wetted surface of the wedge, because it would then be necessary to take ΔC_p into account—which could potentially reach values amounting to about 30% of the value of $C_{p_{\text{Mei}}}$.

In fact, the results presented above suggest certain similarities between impact at constant velocity and impact at variable velocity. Indeed, if at any given time $t = \tau$, the velocity of the wedge in a transient flow $V_{tr}(t)$ is equal to its velocity V_p in a steady flow, then the pressure peaks at points S_{tr2} and S_{p2} are roughly identical (see Fig. 8). Consequently, we may apply a type of quasi-steady approach to reasonably predict the maximum pressure on the body surface. For this purpose, the instantaneous velocity $V(t)$ of the wedge is used together with the $C_{p_{\text{Mei}}}$ formula (Eq. (41)) which is established for a constant-velocity impact to obtain the maximum pressure at any given moment in time (t) of the variable-velocity impact. Thus, the velocity $V(t)$ is considered to be a constant-velocity water entry but it is not equal

to the initial velocity V_0. The change in speed $V(t)$ over time is determined by solving the set of Eqs. (29). This procedure is only used for the peak pressure estimation; elsewhere on the wetted part of the wedge's surface ($S_{tr1} < S < S_{tr2}$), the values of pressure associated with steady and transient flows are different. In this case, instead of Eq. (41), the use of Eq. (36) is required to determine the pressure distribution.

4. Comparison to experimental data

4.1. Description of the experimental set-up

To validate the analytical results presented above, physical experiments have been carried out at the hydraulic research laboratory of Université de Sherbrooke. A diagram of the experimental set-up is shown in Fig. 9. It consists of a vertical shaft of 4 m in length fixed to the bottom of a water channel of 2 m in width, 30 m in length and a maximum depth capacity of 2 m. The water level is set at 1 m to allow drops from a maximum height (hc) of 1.3 m. The wedge is attached to a steel guiding structure that slides along the shaft. As shown in Figs. 9 and 10, the wedge apex is aligned perpendicularly to the longitudinal axis of the water channel.

Five different wedges made from a 19 mm (3/4 inch)-thick plywood board were used. The wedge angle varied from $15°$ to $35°$ as shown in Fig. 11. The wedge walls were rigid and waterproof. All wedges had a square top section of $1.2 \, \text{m} \times 1.2 \, \text{m}$ that could support additional steel parts with masses of 40, 80 and 120 lbm respectively (mass unit of the British Engineering System; 1 kg = 2.205 lbm). Note that because of their respective geometry, the initial wedge weights differed.
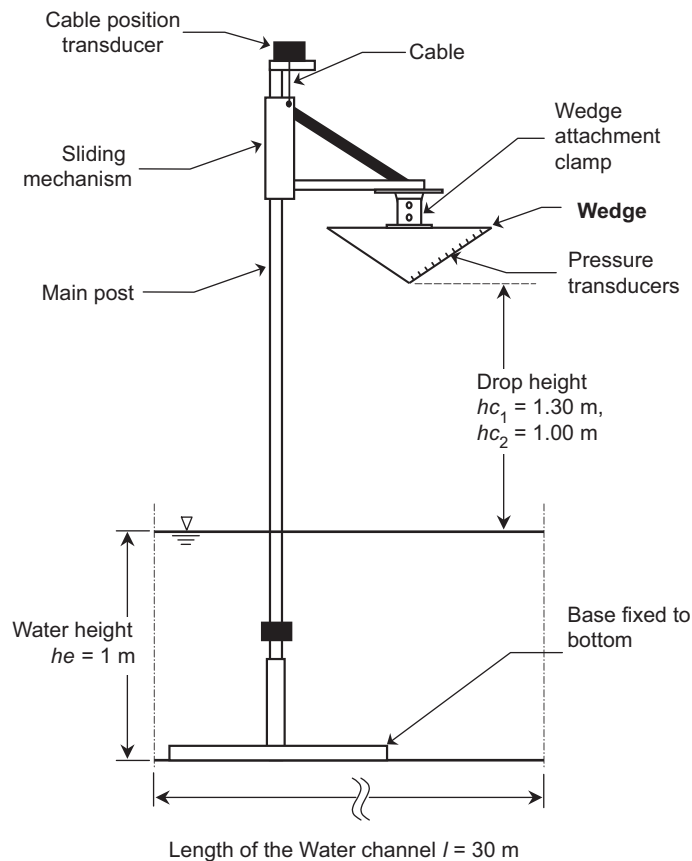
Fig. 9. Diagram of the experimental set-up.
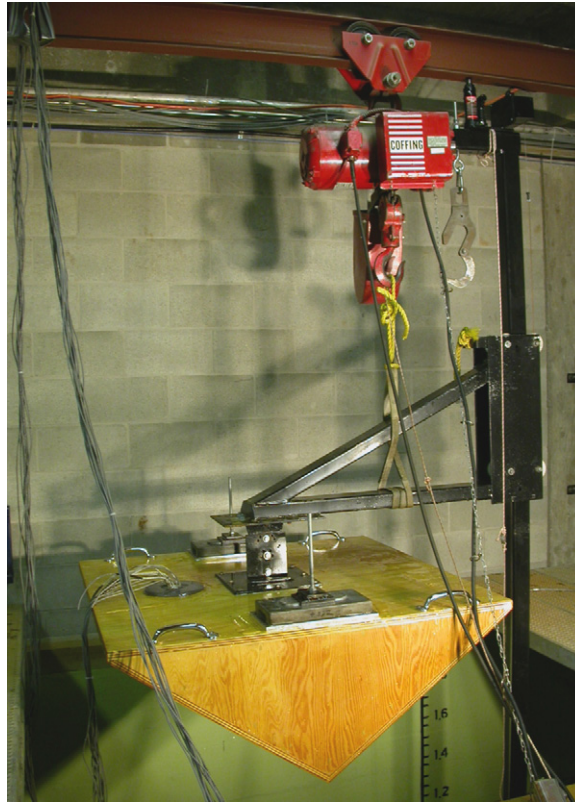
Fig. 10. Photograph of the experimental set-up installed in a water channel.

4.2. Instrumentation

To measure the time variation of the pressure distribution, we used 12 Wheatstone bridge AB/HP Data Instruments pressure transducers. The pressure range of these transducers is 0–500 psi (pressure unit of the British Engineering System: $1 \, \text{psi} = 1 \, \text{lb/in}^2 = 6894.76 \, \text{N/m}^2$) and the diameter of each one is 19 mm. They were distributed along the median line on one side of the wedges. The distance between each transducer was 50 mm, as shown in Fig. 11. They were numbered 1–12, with number 1 located near the wedge apex. The first natural frequency of the transducers was 10 kHz.

To measure the instantaneous position and velocity of the wedge, we used a potentiometric cable extension transducer Celesco model PT5A100S47FR1KM6. Its useful range and precision are provided by the manufacturer and are approximately 2.5 m and $\pm 0.1\%$, respectively. The transducer position raw data were low-pass filtered using a cut-off at 45 Hz to remove spurious noise generated by slight vibrations of the cable. We calculated velocity using a numerical differentiation of the position signal.

Data acquisition was performed using a 16-channel data acquisition system model eDAQ manufactured by Somat Inc. Two 8-channel Low Level Boards designed for the measurement of Wheatstone bridges were used. Full bridge configuration was used. Sampling frequency on every channel was set at 5 kHz.

4.3. Accuracy and sampling frequency

Preliminary tests were carried out to verify measurement accuracy and repeatability. In particular, the objective of these tests was to ensure the sufficiency of the selected sampling frequency. For this purpose, we used a HP35665A signal analyser designed for signal sampling at very high sampling frequencies. Moreover, the most severe impact case was considered, i.e., the impact of a wedge of a deadrise angle $\alpha = 15°$ and a drop height $hc = 1.30$ m. The pressures recorded by the first two transducers closest to the apex of the wedge were analysed. To check the validity of the chosen sampling frequency, we used the well-known Nyquist–Shanon theorem which stipulates that to accurately measure a dynamic signal whose highest natural frequency (Nyquist frequency) is f_n, it is necessary to use a sampling frequency f_s
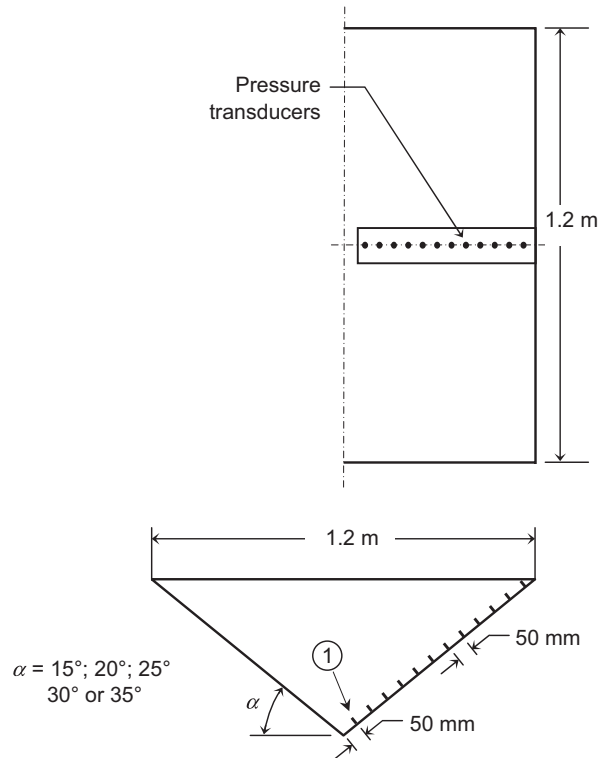
Fig. 11. Wedge description.

that is equal to or greater than $2f_n$. Consequently, to verify that the selected sampling frequency of 5000 Hz is sufficient, we have to ensure that the Nyquist frequency of the studied impact is lower than 2500 Hz. To verify this condition, we considered the signal recorded using the HP analyser to be the raw signal, knowing that its sampling frequency is approximately 260 kHz. Then, to this signal we applied a low-pass numerical filter whose cut-off frequency is 2200 Hz. Figs. 12 and 13 present a comparison between the raw signal and the filtered signal recorded by the transducers no. 1 and 2 for the three identical impact tests.

According to these figures, it is evident that filtering the raw signal at a cut-off frequency of 2200 Hz does not distort the measured pressures. The filtered signal remains satisfactory compared to the raw signal. The computed relative errors related to the peak pressure are approximately 5% for transducer no. 1 and 3% for no. 2. As a result, it is possible to conclude that the highest significant natural frequency of such an impact is lower than 2200 Hz. In fact, we obtain satisfactory results for the filtered signal until cut-off frequencies of about 1500 Hz, where the relative error in the evaluation of the peak pressure starts to become significant (greater than 10% for transducer no. 1.)

Consequently, to properly measure the pressure of such an impact, a sampling frequency equal or greater than twice the cut-off frequency $f_c = 2200$ Hz is sufficient. A sampling at 5000 Hz is thus acceptable and enables us to obtain correct and reliable measurements with a certain degree of confidence. In addition, it is worthwhile to note the satisfactory repeatability of peak pressures for the same configuration and impact parameters (deadrise angle and mass of the wedge and drop height). This is valid for the pressures measured using transducer no. 1 as well for those recorded by transducer no. 2 (see Figs. 12 and 13). We also note that these preliminary results are related to the most severe impact cases encountered during the experiments, namely, a wedge with a deadrise angle $\alpha = 15°$ and a drop height $hc = 1.30$ m. For other configurations (particularly for higher values of angle α), the relative error in the evaluation of maximum pressure associated with the selected sampling frequency decreases noticeably.

4.4. Test configurations

We used several test configurations, based on the modification of one test parameter at a time. The parameters under consideration were:
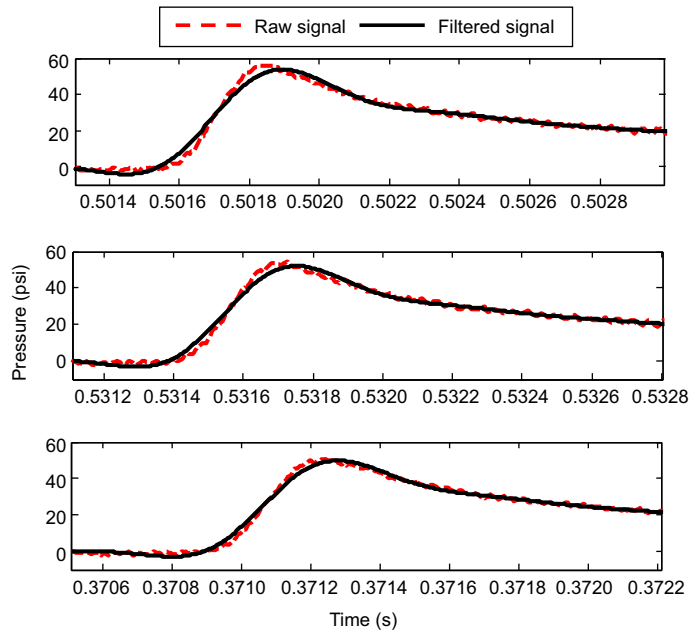
Fig. 12. Comparison between the raw signal and the filtered signal recorded by transducer no. 1 of three identical impacts (wedge's deadrise angle $\alpha = 15°$; wedge mass $m = 89$ kg; drop height $hc = 1.3$ m; sampling frequency of the raw signal $f_s = 262$ kHz; low-pass cut-off frequency $f_c = 2200$ Hz).
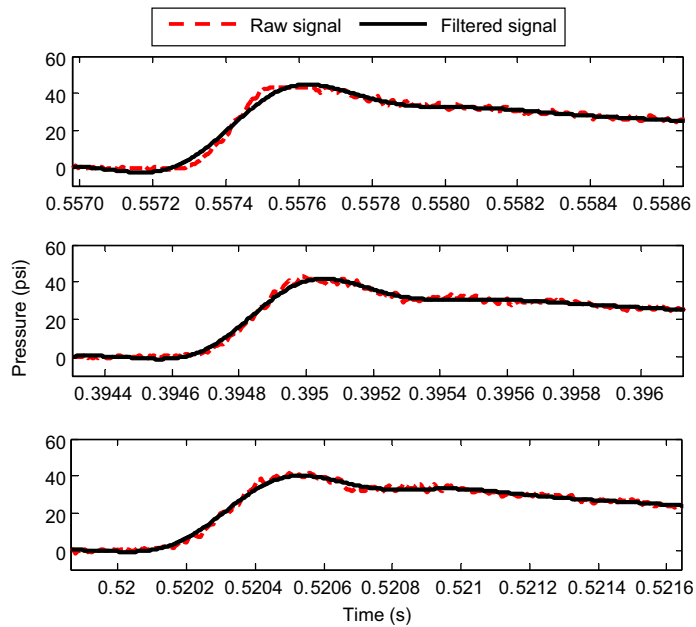
Fig. 13. Comparison between the raw signal and the filtered signal recorded by transducer no. 2 of three identical impacts (wedge's deadrise angle $\alpha = 15°$; wedge mass $m = 89$ kg; drop height $hc = 1.3$ m; sampling frequency of the raw signal $f_s = 262$ kHz; low-pass cut-off frequency $f_c = 2200$ Hz).

  (i) 5 wedge angles: $\alpha = 15°$, $20°$, $25°$, $30°$, $35°$;
 (ii) 2 drop heights: $hc = 1.0$ m et 1.3 m;
(iii) several masses of the slamming body were tested, consisting of the wedge, the sliding mechanism and additional masses details are presented in Table 1.

The wedges were launched vertically from a static position. Five wedges were employed along with four different masses and two drop heights, for a total number of 40 test configurations. To ensure more accurate results, the final data for each configuration were determined from an average of 10 identical tests. It should be noted that measures of identical tests are fairly close (see Figs. 12 and 13). An experimental analysis of uncertainty enabled us to estimate an uncertainty of 7% with a 90% degree of confidence.

4.5. Discussion

Concerning the instantaneous velocity of the wedge, it is possible to observe (according to Fig. 14) a correlation between the analytical model of Zhao et al. (1996) expressed by Eq. (11) and the experimental data on velocity. It is obvious that this model is valid for describing the motion of the wedge at the initial stage of the slamming process, which is of fundamental interest and practical concern because the wedge's velocity and therefore its kinetic energy decrease by over 80% after only 45 ms from the beginning of impact.

To compare the analytical results with the experimental data, we plotted curves expressing the pressure coefficient variation for each of the five test models. Analytically, the coefficient C_p is provided by Eq. (36). Experimentally, C_p is obtained by dividing the values measured by the pressure transducers, using the term $\frac{1}{2}\rho\, V^2(t)$, where $V(t)$ is the instantaneous velocity of the wedge measured by means of the cable position transducer and where ρ denotes the water density.

Table 1
Mass of the experimental slamming bodies

Wedge deadrise angle α	Total mass of the slamming test bodies (kg) (including wedge mass, guiding system mass and additional masses)			
15°	89	107	125	143
20°	89	107	125	143
25°	94	112	130	148
30°	99	117	135	153
35°	104	122	140	158
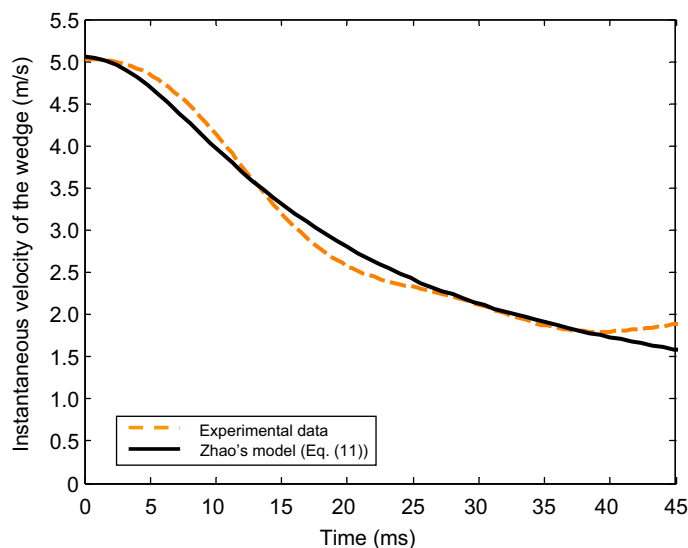
Fig. 14. Comparison of the measured velocity of the wedge to the analytical model of Zhao et al. (1996) (wedge deadrise angle $\alpha = 25°$; wedge mass $m = 94$ kg; drop height $hc = 1.3$ m).
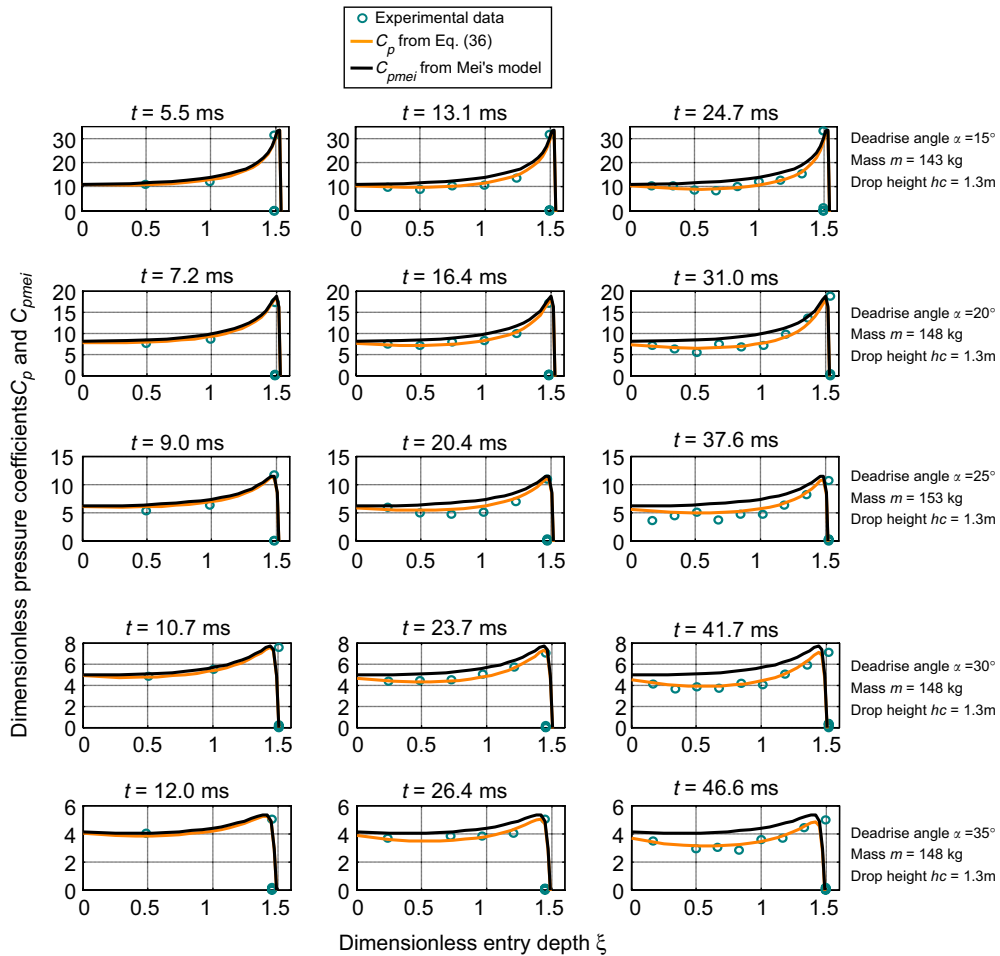
Fig. 15. Comparison of pressure coefficients values obtained from experimental data, Eq. (36) and Mei's model, at different impact times.

To represent the analytical results as well as the experimental data in a dimensionless manner, we plot the variation of the coefficient C_p in terms of the dimensionless entry depth ξ.

Fig. 15 thus represents the values of the pressure coefficient in terms of the dimensionless entry depth ξ at different times of impact. The total uncertainty is estimated to be approximately 10% for C_p and 6% for ξ.

As previously stated, a discrepancy can be observed between the analytical predictions of the dimensionless pressures C_p and $C_{p\mathrm{Mei}}$ (see Fig. 15). This difference is negligible at the beginning of the impact (approximately at $t<1\,\mathrm{ms}$). However, the discrepancy becomes increasingly significant over time. It should be noted, on the other hand, that near the apex and peak pressure, this discrepancy between the two pressure coefficients is less significant than elsewhere on the wetted part of the wedge's surface. We also note that the smaller the deadrise angle α, the sharper the profile of the pressure coefficient and the more significant its peak becomes. According to Fig. 15, it is obvious that Eq. (36) allows the estimation of the pressure coefficient with much more precision than Mei's model (Eq. (41)). However, the latter is more appropriate, with slight uncertainty, for the evaluation of the maximum value of the pressure coefficient $C_{p\mathrm{max}}$.

For this, Fig. 16 demonstrates a comparison between experimental data of the maximum values of the pressure coefficient and the analytical predictions given by Eqs. (36) and (41), the similarity solution and Wagner's asymptotic method (Faltinsen, 2000), for several values of the deadrise angle of the wedge.

Concerning the pressure distribution, Figs. 17–21 show a correlation between the analytical estimates of the slamming pressure and the experimental data collected directly from the pressure transducers. For reasons of clarity, the pressure distribution is represented at only four different moments during the entry phase. We also plot experimental and analytical curves connecting the maximum values of the pressure. Although we note a small
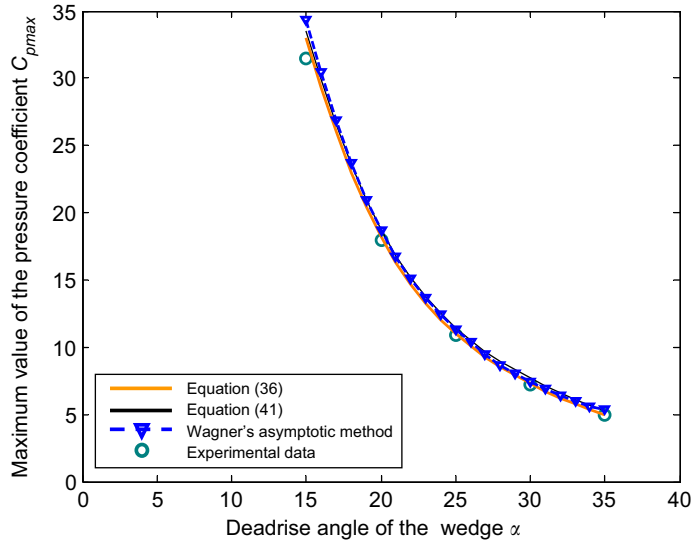
Fig. 16. Variation of the maximum value of the pressure coefficient according to the deadrise angle of wedge α: comparison between the proposed analytical model Eq. (36), Mei's model (Eq. (41)), Wagner's asymptotic method estimations and experimental data (five wedges with deadrise angles uniformly distributed between $15°$ and $35°$; additional mass $m = 120\,\mathrm{lbm}$ has been added to each wedge; drop height $hc = 1.30\,\mathrm{m}$; curves plotted at $t = 30\,\mathrm{ms}$).
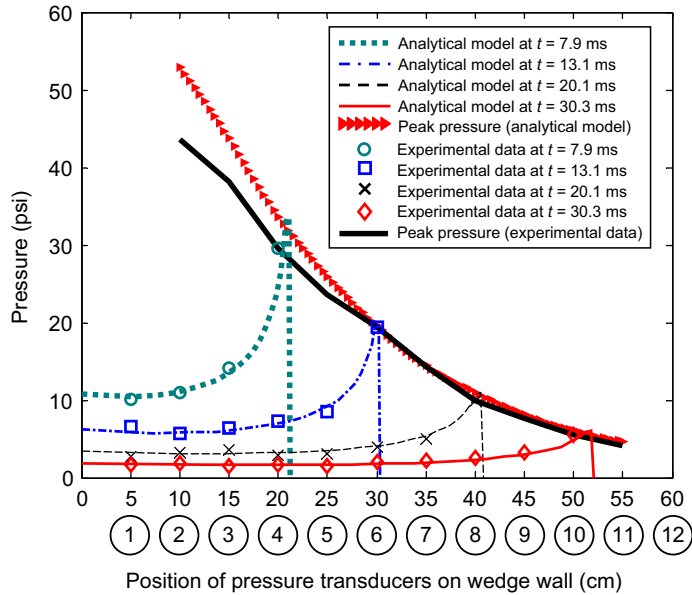
Fig. 17. Comparison between experimental results and analytical model predictions for the pressure distribution on the face of the wedge at different moments of the entry phase (wedge deadrise angle $\alpha = 15°$; wedge mass $m = 143\,\mathrm{kg}$; drop height $hc = 1.3\,\mathrm{m}$).

discrepancy between the analytical and experimental maximum values for pressure upon initial impact ($t < 10\,\mathrm{ms}$) and particularly for a deadrise angle $\alpha = 15°$ or $20°$ (see Figs. 17 and 18), we can nevertheless state that the analytical model provides a satisfactory description of the pressure distribution on a wedge entering water vertically after a free fall from a given drop height.
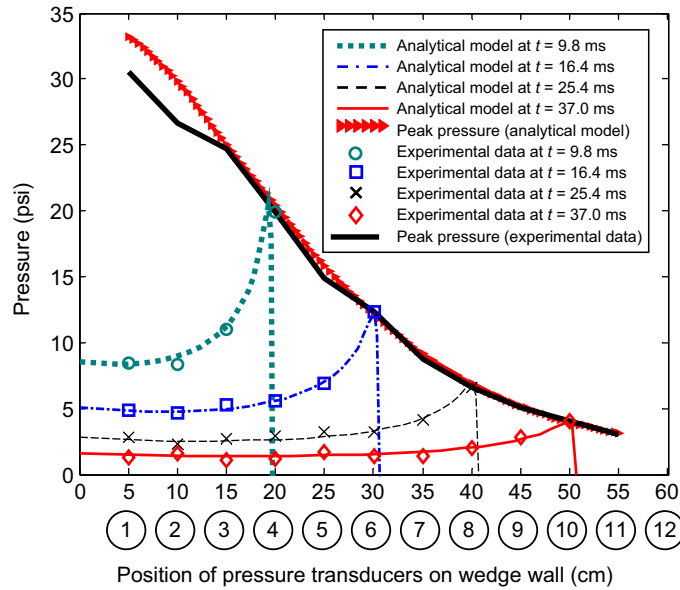
Fig. 18. Comparison between experimental results and analytical model predictions for the pressure distribution on the face of the wedge at different moments of the entry phase (wedge deadrise angle $\alpha = 20°$; wedge mass $m = 143$ kg; drop height $hc = 1.3$ m).
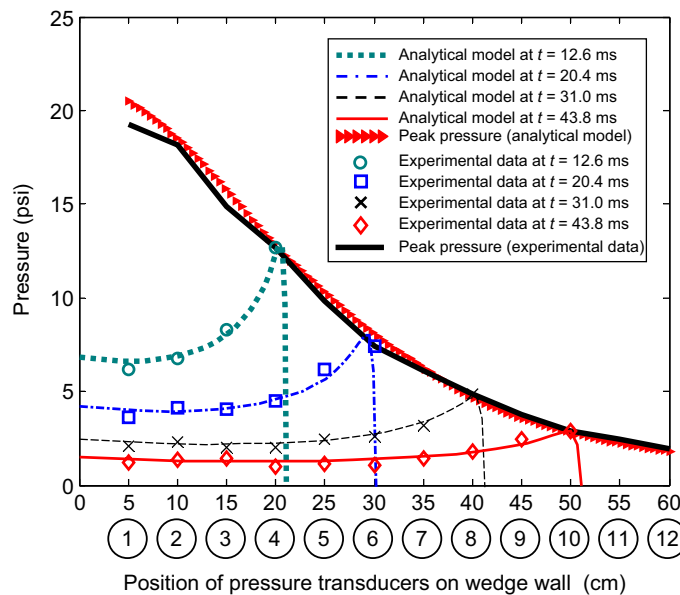
Fig. 19. Comparison between experimental results and analytical model predictions for the pressure distribution on the face of the wedge at different moments of the entry phase (wedge deadrise angle $\alpha = 25°$; wedge mass $m = 148$ kg; drop height $hc = 1.3$ m).

Once the pressure distribution is determined, it is easy to obtain the total slamming force acting on the body. Fig. 22 presents a comparison between analytical results obtained by direct integration of the pressure distribution with respect to the wetted surface of the wedge (see Eq. (37)) and those obtained using Newton's second law (see Eq. (38)). A discrepancy between these two estimation methods is shown in Fig. 22. This difference is due to the error related to the numerical integration of the pressure distribution. However, the maximum value of the force acting on the body can be satisfactorily estimated using either method. A relative error of approximately 5% between the two peaks was recorded.
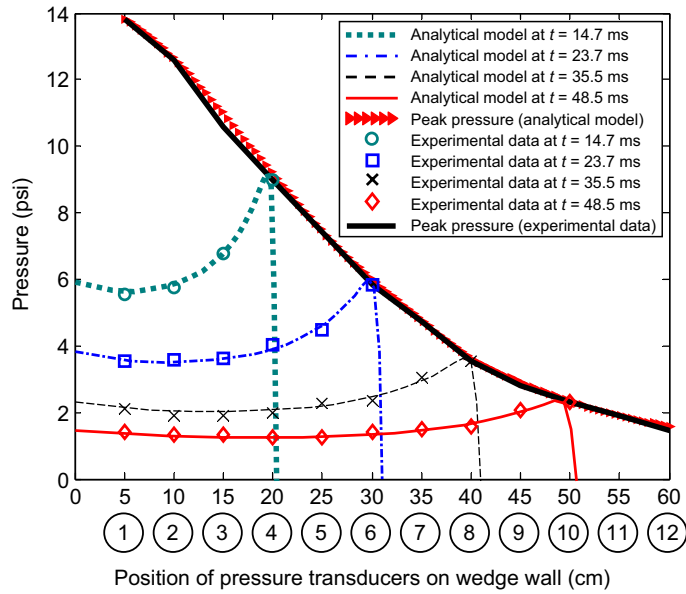
Fig. 20. Comparison between experimental results and analytical model predictions for the pressure distribution on the face of the wedge at different moments of the entry phase (wedge deadrise angle $\alpha = 30°$; wedge mass $m = 153$ kg; drop height $hc = 1.3$ m).
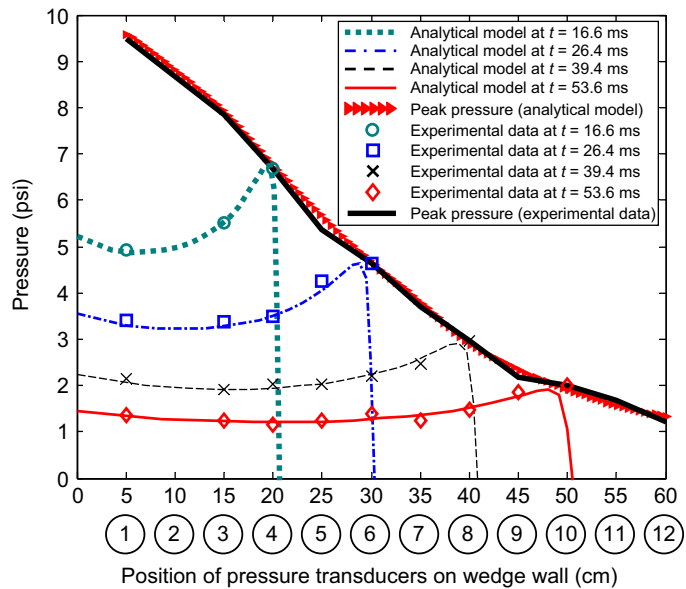
Fig. 21. Comparison between experimental results and analytical model predictions for the pressure distribution on the face of the wedge at different moments of the entry phase (wedge deadrise angle $\alpha = 35°$; mass of the wedge $m = 158$ kg; drop height $hc = 1.3$ m).

5. Conclusion

Unlike most analytical studies carried out on water impact where the velocity of the body is assumed to be constant, the analysis presented in this paper takes into account the effect of body deceleration upon impact. We have developed an analytical model (Eq. (36)), making it possible to evaluate the pressure coefficient in the general case of the symmetrical two-dimensional water impact at variable velocity of a rigid wedge. For this purpose, the free-surface
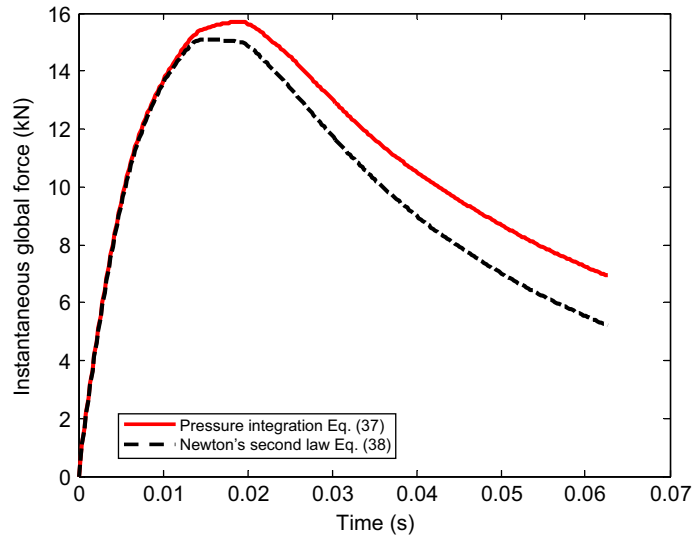
Fig. 22. Comparison between analytical results for the instantaneous force on the dropping wedge obtained using Eqs. (37) and (38) (wedge deadrise angle $\alpha = 30°$; wedge mass $m = 153$ kg; drop height $hc = 1.3$ m).

boundary conditions have been linearised and the body boundary condition has been satisfied in a rigorous manner. The effect of thin-jet flow at the apex of the water splash has, however, been set aside. The solution has been obtained by means of an analytical method based on the conformal mapping technique. Nevertheless, a solution could not have been reached without the use of a different analytical model allowing the estimation of the wedge's instantaneous velocity. For this purpose, we used the Zhao et al. (1996) analytical model. The analytical model presented herein highlights the fact that the pressure coefficient roughly preserves the same values at the pressure peak and at the wedge apex. Otherwise, between these two positions the values of the coefficient decrease over time and are dependent on certain parameters of impact, such as body mass and initial impact velocity. This constitutes the main difference between an impact at constant velocity and an impact at variable velocity.

The analytical results have been confirmed by successfully comparing them to experimental data collected from physical tests carried out on several wedges and with different configurations (several masses, drop heights and deadrise angles). This analytical method represents a significant practical tool, making it possible to evaluate the pressure distribution and the slamming force without having to resort to complex nonlinear numerical simulations.

References

Armand, J.-L., Cointe, R., 1987. Hydrodynamic impact analysis of a cylinder. ASME Journal of Offshore Mechanics and Arctic Engineering 109, 237–243.

Cappelli, A.P., Wilkinson, J.P.D., 1967. Study of Apollo Water Impact, vol 2: Dynamic Response of Shells of Revolution During Vertical Impact into Water—No Interaction. North American Aviation, Inc., Space Division, Library of Spacecraft Center, Houston, Texas, USA.

De Divitiis, N., de Socio, L.M., 2002. Impact of floats on water. Journal of Fluid Mechanics 471, 365–379.

Dobrovolskaya, Z.N., 1969. On some problems of similarity flow of fluid with a free surface. Journal of Fluid Mechanics 36, 805–829.

Fraenkel, L.E., Keady, G., 2004. On the entry of a wedge into water: the thin wedge and an all-purpose boundary layer equation. Journal of Engineering Mathematics 48, 219–252.

Fraenkel, L.E., McLeod, J.B., 1997. Some results for the entry of a blunt wedge into water. Philosophical Transactions of the Royal Society of London A 355, 523–535.

Faltinsen, O.M., 2000. Sea Loads on High-speed Marine Vehicles. Kompendium, Department of Marine Hydrodynamics, Marine Technology Center, Norwegian University of Science and Technology Trondheim, Norway.

Faltinsen, O.M., 2002. Water entry of a wedge with finite deadrise angle. Journal of Ship Research 46, 39–51.

Faltinsen, O.M., Landrini, M., Greco, M., 2004. Slamming in marine applications. Journal of Engineering Mathematics 48, 187–217.

Howison, S.D., Ockendon, J.R., Wilson, S.K., 1991. Incompressible water-entry problems at small deadrise angles. Journal of Fluid Mechanics 222, 215–230.

Hughes, O.F., 1972. Solution of the wedge entry problem by numerical conformal mapping. Journal of Fluid Mechanics 56, 173–192.

Korobkin, A.A., 1997. Asymptotic theory of liquid–solid impact. Philosophical Transactions of the Royal Society of London A 355, 507–522.

Korobkin, A.A., 2004. Analytical models of water impact. European Journal of Applied Mathematics 15, 821–838.

Korobkin, A.A., Pukhnachov, V.V., 1988. Initial stage of water impact. Annual Review of Fluid Mechanics 20, 185–195.

Korobkin, A.A., Scolan, Y.-M., 2006. Three-dimensional theory of water impact. Part 2. Linearised Wagner problem. Journal of Fluid Mechanics 549, 343–373.

Li, T., Sigimura, T., 1967. Study of Apollo Water Impact, vol 1: Hydrodynamic Analysis of Apollo Water Impact. North American Aviation, Inc., Space Division, Library of Spacecraft Center, Houston, Texas, USA.

Mei, X., Lui, Y., Yue, D.K.P., 1999. On the water impact of general two-dimensional sections. Applied Ocean Research 21, 1–15.

Meyerhoff, W.K., 1970. Added masses of thin rectangular plates calculated from potential theory. Journal of Ship Research, 100–111.

Newman, J.N., 1977. Marine Hydrodynamics. The MIT Press, Cambridge, MA.

Payne, P.R., 1988. Design of High-Speed Boats, vol. 1. Planing. Fishergate, Inc., Maryland.

Scolan, Y.-M., Korobkin, A.A., 2001. Three-dimensional theory of water impact. Part 1. Inverse Wagner problem. Journal of Fluid Mechanics 440, 293–329.

Troesch, A.W., Kang, C.-G., 1987. Hydrodynamic impact loads on three-dimensional bodies. In Proceedings of the 16th Symposium on Naval Hydrodynamics, Berkeley, CA, USA.

Troesch, A.W., Kang, C.-G., 1990. Evaluation of impact loads associated with flare slamming. Journal of The Society of Naval Architects of Korea 27 (3), 56.

von Karman, T., 1929. The impact on seaplane floats during landing. Technical Notes, National Advisory Committee for Aeronautics.

Wagner, H., 1936. Phenomena associated with impacts and sliding on liquid surfaces. NACA Library, Langley Aeronautical Laboratory. Translation of: Wagner, H., 1932. Über stoß und gleitvorgänge an der oberfläche von flüssigkeiten. Zeitschrift für angewandte Mathematik und Mechanik 12, 193–215.

Yu, Y.-T., 1945. Virtual masses of rectangular plates and parallelepipeds in water. Journal of Applied Physics 16, 724–729.

Zhao, R., Faltinsen, O.M., 1993. Water entry of two-dimensional bodies. Journal of Fluid Mechanics 246, 593–612.

Zhao, R., Faltinsen, O.M., Aarsnes, J., 1996. Water entry of arbitrary two-dimensional sections with and without flow separation. In: Proceedings of the 21st Symposium on Naval Hydrodynamics, Trondheim, Norway, National Academy Press, Washington, DC, USA.